Electronic structure of CdTe(110) as studied by angle-resolved photoemission

H. Qu, P. O. Nilsson, J. Kanski, and L. Ilver
Department of Physics, Chalmers University of Technology, S-412 96 Göteborg, Sweden
(Received 26 August 1988)

Photoemission energy distributions from cleaved CdTe(110) surfaces have been measured in the $\bar{\Gamma}\bar{X}$ and $\bar{\Gamma}\bar{Y}$ azimuths for photon energies of 16.8 and 21.2 eV. Using a semiempirical band calculation, we were able to sort out the origin of the observed structures in terms of direct and indirect excitations in the bulk as well as contributions from the surface.

I. INTRODUCTION

There has been great interest in recent years in the electronic structure of CdTe and its alloys. The latter include those with transition metals (e.g., Mn) showing interesting magnetic phenomena. For further studies of these materials, it is of great importance that the electronic structure of pure CdTe and its surfaces is well known. Although several investigations in this area have been reported in literature, there are still many uncertainties.

The aim of the present paper is to identify all observed structures in photoelectron spectra. "Band mapping," based on photoelectron spectroscopy, has been quite successful for metals, the spectra of which are dominated by direct transitions in the bulk. Semiconductor spectra are often more complicated, showing considerable contribution from "density-of-states effects" and surface states (resonances). We would also like to stress at this point that the electronic structure established through photoemission experiments is not the same as the ground-state band structure usually presented in literature. So, for instance, energy differences of the order of 1 eV may be expected due to many-body effects in the excited state.[1]

II. BAND-STRUCTURE CALCULATION

The observed features in photoelectron energy distribution curves (EDC's) often show a complicated pattern as a function of the electron detection angle. To be able to interpret the origin of such data—in particular the off-normal emission—it is of great help to first compare with calculated peak positions from a band structure. The linear combination of atomic orbitals (LCAO) scheme by Chadi and Cohen[2] provides a possibility to obtain a semiempirical band structure in a simple way. We have previously applied this scheme with good results, e.g., on calculations of Auger spectra from GaAs.[3] The application to CdTe requires some generalizations, however. Firstly, relativistic effects are so strong that they should not be neglected. Secondly, the enclosure of second-neighbor interactions turned out to improve some details. With respect to the relativistic effects, the Darwin and mass-velocity contributions will shift and distort the bands, effects which can be absorbed in the original parameters of the scheme. The spin-orbit interaction, however, removes degeneracies and has to be incorporated explicitly in the calculations:

$$H = H_{\text{orbit}} + H_{\text{s.o.}} .$$

Within the LCAO formalism we write for the spin-orbit part,

$$H_{\text{s.o.}} = \sum_{i,\mu,\mu',\sigma,\sigma'} c^{\dagger}_{i\mu\sigma} c_{i\mu'\sigma'} \langle \mu\sigma | \xi(r) \mathbf{L}\cdot\mathbf{S} | \mu'\sigma' \rangle ,$$

where

$$\xi(r) = \frac{h^2}{2m^2c^2} \frac{dV(r)}{dr} .$$

Here, i is the site index, μ the type of orbital, and σ the spin quantum number. Because of the localized nature of this interaction only intra-atomic terms are included. The potential $V(r)$ is assumed to be spherically symmetric. We take ξ outside the integral and consider its average as a parameter of the scheme. By the inclusion of spin-orbit interaction, the dimension of the Hamiltonian matrix is thus doubled. As we have not found the evaluation of the new determinant in literature, we give the explicit results in Appendix A. In the original Chadi-Cohen and Harrison LCAO formulation,[2,4] there are eight parameters (taking the two types of s-p overlaps to be equal). Two parameters are now added, namely for the spin-orbit interaction of Cd and Te, respectively. These ten parameters were first fitted to the band structure of Humphrey *et al.*[5] at the critical points Γ, X, K, and L. A standard deviation of about 0.5 eV was found. For a semiconductor we expect deviations in excitation spectra from even a good ground-state band structure.[1] Not surprisingly, we thus had to further adjust the parameters to get optimal agreement with our experimental results. Still, there were deviations between experiment and theory for specific emission angles, which could be attributed to approximations in the band calculation. In particular, a strong minimum along the ΓKX direction in the fourth band [counted from the valence-band maximum (VBM)] could not be fully reproduced. We therefore extended the interaction to next nearest neighbors. It turned out that the important interaction element is $V_{pp\sigma}$ between the same kind of atoms along the [110]

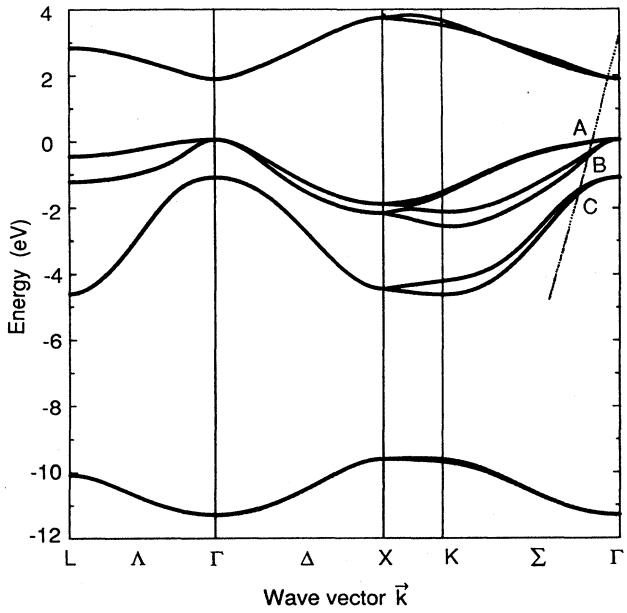

FIG. 1. The optimized band structure of CdTe calculated in a LCAO scheme including spin-orbit coupling and some second-neighbor interactions (see the text).

directions (see Appendix B). For the total Hamiltonian we now write

$$H = H_{\text{orbit}} + H_{\text{s.o.}} + H_{pp\sigma} .$$

The resulting band structure is displayed in Fig. 1. Only the energy region between 0 and -5 eV is used for the following analysis. The conduction bands are not very accurate because of the limited basis set. The low-lying valence bands are in reality distorted by the presence of the Cd $4d$ states around -10 eV.

III. EXPERIMENT

The undoped CdTe crystal was obtained from MCP Electronic Materials, Ltd. A clean, mirrorlike (110) surface was produced by cleavage in ultrahigh vacuum (10^{-10} torr). The measurements were carried out in an ADES 400 system with the analyzer movable in one plane. Except for the x,y,z translations, the sample manipulator allowed for two rotations: around a vertical axis through the sample (variation in the light incident angle) and around one horizontal axis (variation of electron azimuthal angle). No rotation was possible around the horizontal axis in the plane of the sample surface, and consequently it was not possible to make any fine adjustment of the surface normal into the rotation plane of the energy analyzer. The angle between this plane and the surface normal was typically 2° or less. He I (21.2 eV) and Ne I (16.8 eV) resonance lines were used for excitation. Spectra were taken for emission angles along the $\bar{\Gamma}\bar{X}$ and $\bar{\Gamma}\bar{Y}$ azimuths in the surface Brillouin zone with an angular resolution of ±2°. The azimuthal orientation was determined by low-energy electron diffraction (LEED), which showed a sharp rectangular pattern with little background intensity. The light incidence angle was kept constant at 47° relative to the surface normal. The results were well reproducible between different cleavages.

IV. RESULTS AND DISCUSSION

Eastman *et al.*[6] were the first ones to get a good overall picture of the valence band of CdTe. They established from their angle-integrated data the correct width of the valence band. This was found to be considerably larger than that obtained earlier by empirical pseudopotential calculations. Ebina and Takahashi[7] reported on the first angle-resolved studies. Their data (restricted to 21.2 eV in the $\bar{\Gamma}\bar{X}$, $\bar{\Gamma}\bar{Y}$, and $\bar{\Gamma}\bar{M}$ directions) are on the whole in agreement with ours, showing a rich and complex structure. Their analysis was not detailed, but the possible existence of a surface state was pointed out. Pessa *et al.*[8] made a more limited study of angle-resolved photoemission at 21.2 eV on films grown by atomic layer epitaxy. Their main conclusion was that a peak observed at 0.33 eV below the VBM by Ebina and Takahashi is due to an intrinsic surface state. Humphrey *et al.*[5] reported angle-resolved data for polar angles less than 20° in the $\bar{\Gamma}\bar{X}$ and $\bar{\Gamma}\bar{Y}$ directions. The interpretation was given in terms of bulk transitions only. The authors compared with calculated peak positions using a nonlocal pseudopotential method. They obtained very good agreement but the results differ from ours. In particular, in the $\bar{\Gamma}\bar{Y}$ direction the E versus $\mathbf{k}_{\parallel}$ dispersion is qualitatively different. Although we do not have any conclusive explanation for this discrepancy, we would like to point out two complications. Firstly, it is sometimes hard to extract accurate peak dispersions from experimental data due to overlapping features, faint structures, etc. Theoretical predictions are then of great help. Secondly, the representation of the final state may be important. We used free-electron parabolas while Humphrey *et al.*[5] used band-calculation results. For the moment it is not clear, however, if this difference is important for the conflicting results. Another discrepancy concerns the absence of observable spin-orbit splitting in both experiment and theory of Humphrey *et al.* As will be discussed later, this splitting shows up clearly in our data. Finally, Magnusson and Flodström[9] have reported on extensive angular studies along the surface Brillouin edges for photon energies in the range 13–26 eV. The valence band, calculated by a linear augmented-plane-wave (LAPW) scheme, was well reproduced if umklapp excitations were included. Four different surface states were extracted from the data. In particular, the surface state reported by Ebina and Takahashi[7] just below the VBM was confirmed by the lack of dispersion with $\mathbf{k}_{\perp}$.

Our measured EDC's are displayed in Fig. 2 for the $\bar{\Gamma}\bar{X}$ and $\bar{\Gamma}\bar{Y}$ azimuths. The energy scale gives the binding energy relative to the Fermi level, which was determined to be 1.15 eV above the VBM. The normal emission spectra in the two azimuths appear somewhat different, since they in fact represent off-normal emission due to the above-mentioned limitations in angular adjustments. Also, the photon angle of incidence is in different azimuthal planes giving rise to different excitation proba-

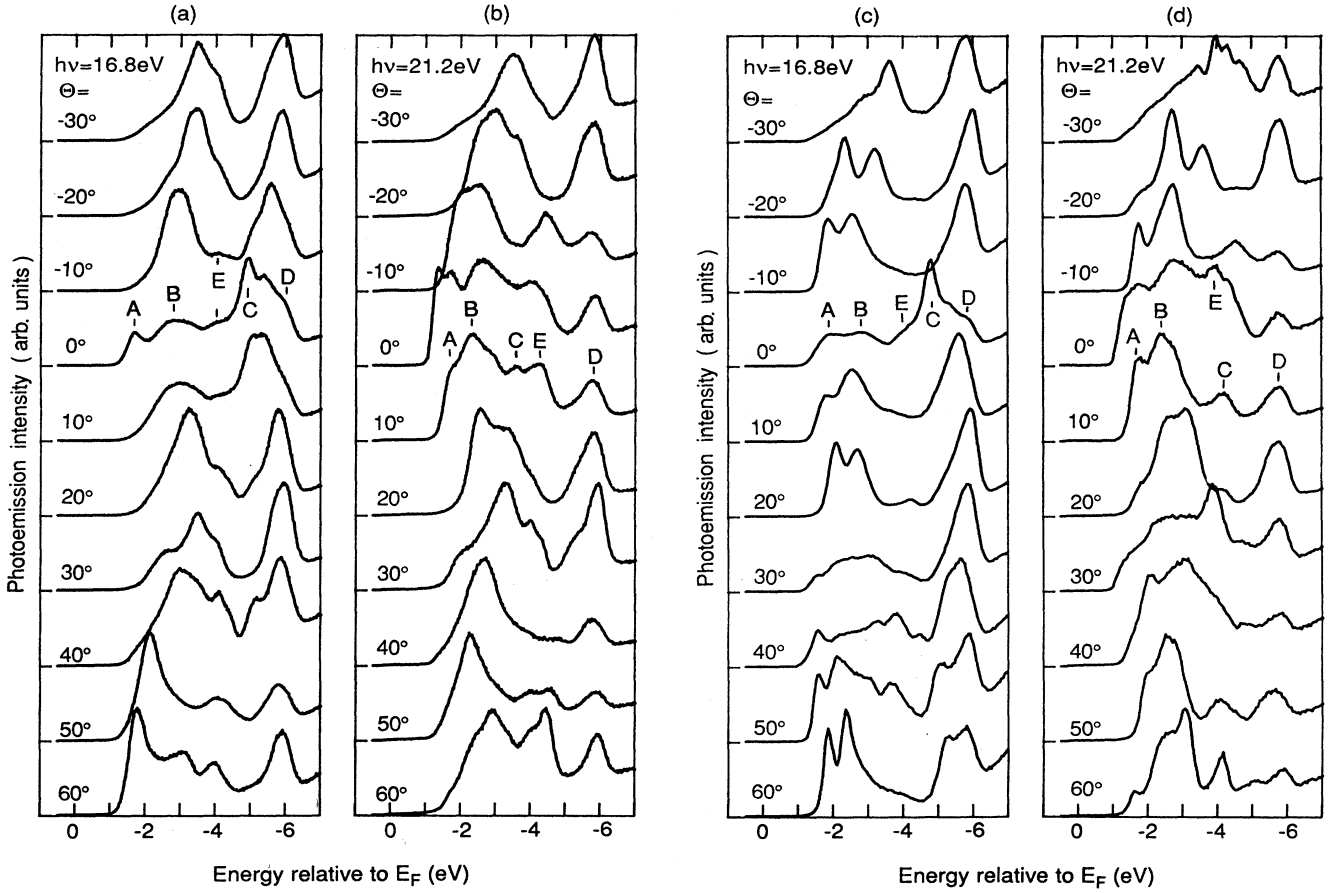

FIG. 2. Measured energy distribution curves (EDC's) for 16.8- and 21.2-eV photon energies and detection angles in the $\bar{\Gamma}\bar{X}$, (a) and (b), and $\bar{\Gamma}\bar{Y}$, (c) and (d), azimuths.

bilities. The positions of *all* observed features as a function of detection angle have been condensed into "structure plots" (Fig. 3). Here, the solid circles refer to clear peaks in the spectra while the open circles represent faint structures such as shoulders, kinks, etc.

As a guide for our interpretation, we start with the band-structure calculation described above. From these bands, structure plots were calculated assuming direct transitions in the bulk (see Fig. 3). Note that the zero of the energy scale is put at the VBM. As the final states are not well represented in our simple band calculation, we have used free-electron bands for the structure-plot calculation, keeping in mind that this might be a crude approximation in certain energy regions. Optimum agreement was found with the extrapolated bottom of the free-electron band at 4.0 eV below the VBM. A work function of 5.43 eV was employed. Using this theoretical structure plot we first identified the experimental peaks corresponding to direct bulk transitions.

Theoretical structure plots were first constructed using "primary excitations" only (see Fig. 3). With this we mean that an excitation from a Bloch state $\mathbf{k}$ to a free-electron state $E_f \sim |\mathbf{k}-\mathbf{g}|^2$ takes place via a momentum transfer $\mathbf{g}$. Around the surface normal [110] only $\mathbf{g}=(2,2,0)$ is active, while at large angles also (1,1,1)- and (2,0,0)-type vectors contribute. In this way we can identify the interband transitions denoted *A*, *B*, and *C* (see Figs. 2 and 3). Each of these three is spin-orbit split.

The origin of the transitions at normal emission is clear from the band structure in Fig. 1, where the photoelectron state has been translated down by the photon energy. For off-normal emission, however, it is not immediately clear what we detect. To analyze this we have traced the direct bulk transitions in $\mathbf{k}$ space (see Fig. 4). As seen, when increasing the detection angle the transitions move away from the normal and approach a Brillouin zone boundary at high detection angles ($\sim 30°-40°$). When passing the boundary (the *KLU* line in the $\bar{\Gamma}\bar{Y}$ azimuth and the *WXW* line in the $\bar{\Gamma}\bar{X}$ azimuth) the binding energies in the structure plot have to go through extreme values due to symmetry reasons. In accordance with this we observe minima in Fig. 3. The $\mathbf{k}_{\parallel}$ values at these points of "bending over" are experimentally well reproduced in the structure plots.

In the real band structure, the photoelectron bands are not strictly free-electron states, but are better described as "nearly-free-electron-like." In the first approximation we keep the free-electron dispersion $E_f \sim |\mathbf{k}-\mathbf{g}|^2$ but consider a wave function containing a mixture of plane waves of various $\mathbf{g}$ vectors. This means that the momentum transfer $\mathbf{g}$ at the excitation need not be equal to the $\mathbf{g}$ vector in $E_f \sim |\mathbf{k}-\mathbf{g}|^2$. The deviation from free-electron

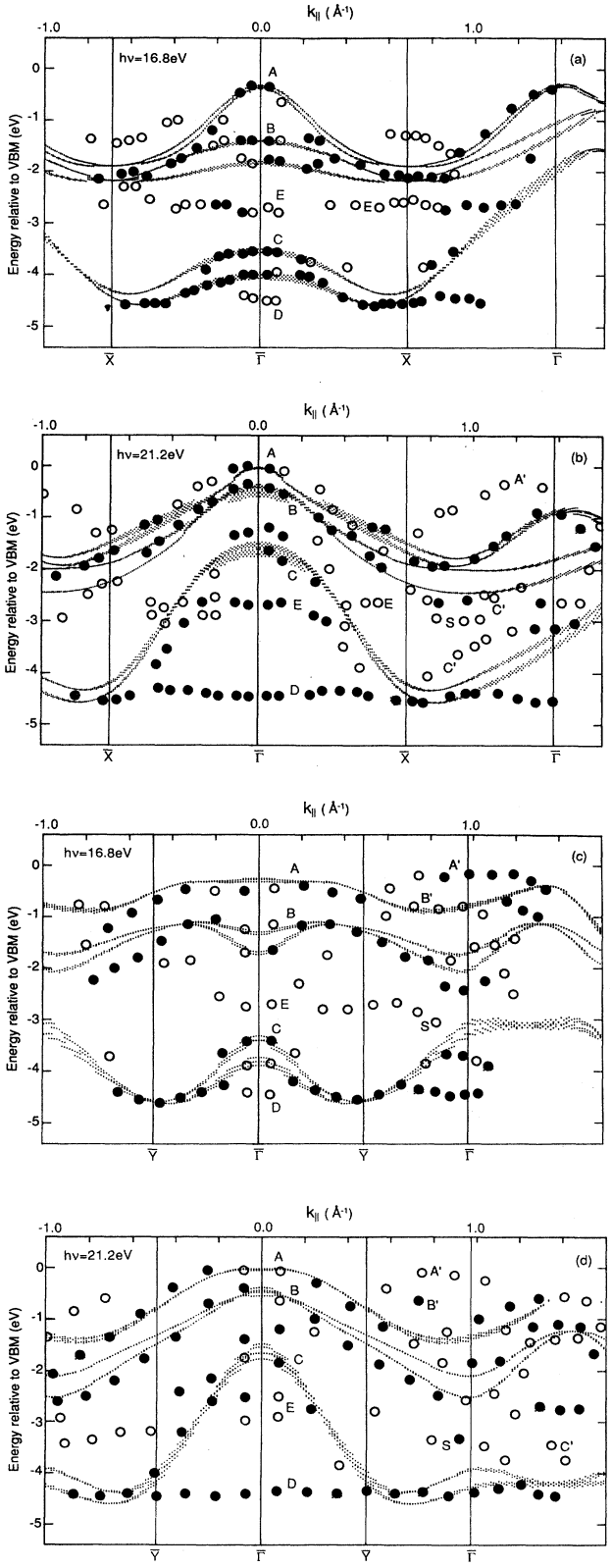

FIG. 3. Experimental structure plots showing the energies of clear peaks (●) and fainter structures (○) in the $\bar{\Gamma}\bar{X}$ and $\bar{\Gamma}\bar{Y}$ azimuths. The theoretical structure plot is shown as broad, dotted lines. A total width of 0.5 eV was used for the final bands.

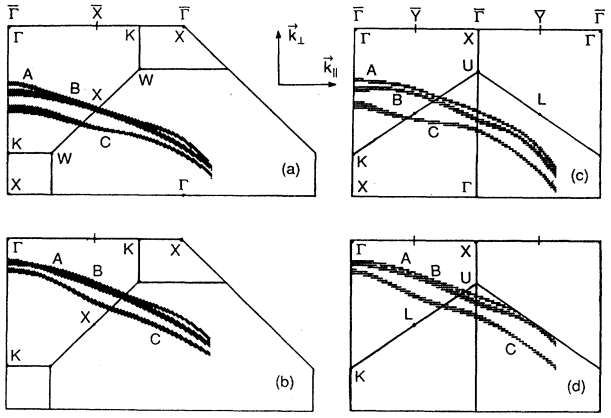

FIG. 4. Theoretical **k**-space locations of direct bulk transitions. A total width of 0.5 eV was used for the final bands.

behavior may also result in non-negligible distortions of the energy bands. In the first place, these are rigid shifts, at least away from band gaps and band crossings. Such shifts depend, in general, on the **g** vector involved, which introduces some uncertainties in calculations of the discussed "secondary emission." In Figs. 3(b), 3(c), and 3(d) the structures *A'*, *B'*, and *C'* could, in principle, be interpreted as secondary emission. Note that, in our case, these transitions introduce the same periodicity in the structure plots as surface-related excitations, and Ebina and Takahashi[7] assign them as such as discussed above. A third possibility, discussed below, is "indirect" transitions, which can, in principle, also explain the structures *D* and *E*.

The pronounced structure *D* in the experimental curves cannot be identified as a direct bulk transition between sharp bands. The observed dispersion of this state is very small but not zero. We propose that the transitions are still direct in the sense that the momentum change of the electron is supplied by the photon and rigid crystal lattice only. We believe that the factors giving rise to the observed "density-of-states behavior," i.e., small dispersion, are the high density of the initial states in combination with large lifetime of the photoelectron.[10].

Structure plots were calculated [see Figs. 5(a) and 5(b)],

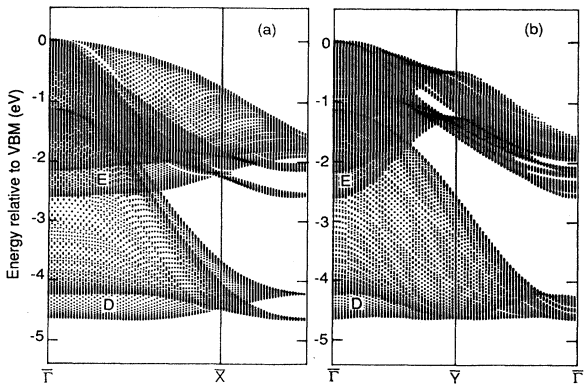

FIG. 5. Theoretical structure plot of bulk transitions into very broad final states. Only $\mathbf{g}=(2,2,0)$ was used.

assuming a very large energy broadening for the photoelectron. Here only $\mathbf{g}=(2,2,0)$ was used. Applying all possible $\mathbf{g}$ vectors will produce a pattern with one period for the distance $\bar{\Gamma}$-$\bar{\Gamma}$. The result is independent of the photon energy but depends on the detection angle because of the direct nature of the excitation. In a model assuming true indirect (phonon-assisted) transitions, the result would also be independent of the emission angle. The shadowing in the figures indicates the density of available states. We observe theoretically for the D structure two almost-dispersion-free peaks around 4.6-eV binding energy. Assuming a realistic hole broadening (say, 0.5 eV) these two peaks would merge into one peak as found experimentally. The small, but non-negligible, experimental and theoretical dispersions do not agree in detail. As this is a very small effect and can thus be influenced by details of the band structure, intensities, etc., we do not judge the disagreement as a disqualification of our model. According to Fig. 6, the main contribution from the excitation comes from large areas in the outer part of the Brillouin zone. The structure E around 2.8 eV below VBM at the center of the zone is tentatively interpreted in the same manner as structure D. The density-of-states calculation in Fig. 5 shows an edge in this region. As mentioned above, the structures A', B', and C' are also candidates for such transitions.

The surface state reported just below the VBM by several authors (see above) cannot be clearly identified at normal emission for our photon energies due to the interference with bulk interband transitions. Like Ebina and Takahashi,[7] we do observe a structure at off-normal emission with the periodicity of the surface Brillouin zone. However, we cannot in the present data distinguish this interpretation from indirect transitions as discussed above.

The feature S in Fig. 3 appears in a gap in the projected bulk states (see Fig. 5). It cannot simply be interpreted using the bulk states, and is thus a candidate for a surface-states interpretation. It might be associated with the surface-state S_3 found around the M point by Magnusson and Flodström.[9]

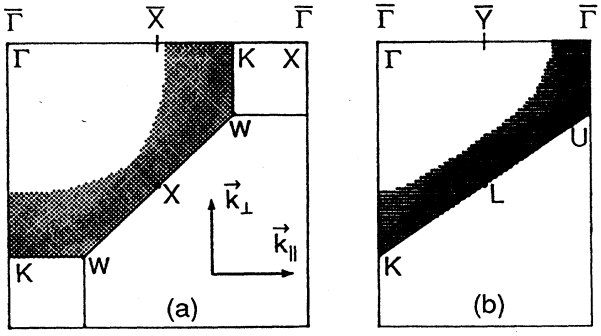

FIG. 6. Theoretical $\mathbf{k}$-space locations of direct bulk transitions from the peak 5 eV (± 0.25 eV) into broad electron states. Only $\mathbf{g}=(2,2,0)$ was used.

V. SUMMARY

Angle-resolved photoemission from cleaved CdTe (110) was studied in some detail in the $\bar{\Gamma}\bar{X}$ and $\bar{\Gamma}\bar{Y}$ directions for photon energies of 16.8 and 21.2 eV. The main pieces of structure were identified as direct transitions between bulk bands. The photoemission bulk band structure was established in this way down to 5 eV below the VBM. Other features in the spectra were found to originate from transitions sampling a large part of the Brillouin zone as a combined effect of the large damping of the photoelectron and the high density of hole states. A surface state was identified in the region 2.8–3.2 eV below the VBM.

ACKNOWLEDGMENT

This work has been supported by grants from the Swedish Natural Science Research Council.

APPENDIX A

The original LCAO version[2,4] was entended to include spin-orbit interactions. We find that out of the $16\times 16=256$ elements of the total Hamiltonian, only 24 spin-orbit terms are different from zero. The symmetry observed in these parameters originates from the general property of invariance of the Hamiltonian under time inversion. Note that we do not have any space inversion for the zinc-blende structure. The spin matrix elements are $\mathbf{k}$ independent, but depend on the spin quantization axis which, for simplicity, has been chosen in the z direction. Identical results are obtained for the cation and anion, as we are using a local approximation, so we give only 12 of the elements here. The first six are as follows:

$$\langle p_x\sigma_\pm|H_{\text{s.o.}}|p_y\sigma_\pm\rangle=\mp ih\ ,$$

$$\langle p_x\sigma_\mp|H_{\text{s.o.}}|p_z\sigma_\pm\rangle=\mp h\ ,$$

$$\langle p_y\sigma_\mp|H_{\text{s.o.}}|p_z\sigma_\pm\rangle=-ih\ ,$$

where h is a parameter of the scheme.

The other six nonzero elements are obtained through the requirement that the matrix has to be Hermitian.

APPENDIX B

Our band calculation guarantees only that the energies are correct at the critical points used for fitting. The experimental data indicate that the fourth band from the VBM along the ΓKX direction has a deeper minimum than is possible to reproduce by the standard LCAO scheme. Including second-neighbor interactions, however, gives in principle the possibility to also vary the curvature of the bands. There are then four new overlap integrals to consider, namely $V_{ss\sigma}$, $V_{sp\sigma}$, $V_{pp\sigma}$, and $V_{pp\pi}$. For our purpose, i.e., to reproduce the bands better along ΓKX, we found $V_{pp\sigma}$ to be the important parameter. A qualitative picture of this contribution is obtained if we consider the $V_{pp\sigma}$ interactions in the diagonal terms only.

We then arrive at a contributions as follows:

$$E = \tfrac{1}{2} V_{pp\sigma} \cos(kd)[2\sin(kd)+1] .$$

This function has a minimum about halfway along the ΓK distance. This effect survives qualitatively in the full calculation and improves the band structure to the extent that it can be used to identify the observed structures more definitely.

[1]M. S. Hybertsson and S. G. Louie, Phys. Rev. B **34**, 5390 (1986).
[2]D. Chadi and M. L. Cohen, Phys. Status Solidi B **68**, 405 (1975).
[3]S. P. Svensson, P. O. Nilsson, and T. G. Andersson, Phys. Rev. B **31**, 5257 (1985).
[4]W. A. Harrison, *Electronic Structure and the Properties of Solids* (Freeman, San Francisco, 1980), p.77
[5]T. P. Humphrey, G. P. Srivastava, and R. H. Williams, J. Phys. C **19**, 1259 (1986).
[6]D. E. Eastman, W. D. Grobman, J. L. Freeouf, and M. Erbudak, Phys. Rev. B **9**, 3473 (1974).
[7]A. Ebina and T. Takahashi, J. Cryst. Growth **59**, 51 (1982).
[8]M. Pessa, P. Huttunen, and M. A. Herman, J. Appl. Phys. **54**, 6047 (1983).
[9]K. O. Magnusson and S. A. Flodström, Ph. D. thesis, Lund University, 1987 (ISBN No. 91-7900-352-4).
[10]T. Grandke, I. Ley, and M. Cardona, Phys. Rev. B **18**, 3847 (1978).